Signal Processing 189 (2021) 108291

Contents lists available at ScienceDirect

Signal Processing

journal homepage: www.elsevier.com/locate/sigpro

Operator theory-based computation of linear canonical transforms

Aykut Koç[a,b,*], Haldun M. Ozaktas[a]

[a] Department of Electrical and Electronics Engineering, Bilkent University, Bilkent, Ankara, Turkey
[b] National Magnetic Resonance Research Center (UMRAM), Bilkent University, Bilkent, Ankara, Turkey

ARTICLE INFO

Article history:
Received 30 June 2020
Revised 14 July 2021
Accepted 11 August 2021
Available online 12 August 2021

Keywords:
Linear canonical transform (LCT)
Fractional Fourier transform (FRFT)
Operator theory
Discrete transforms
Hyperdifferential operators

ABSTRACT

Linear canonical transforms (LCTs) are extensively used in many areas of science and engineering with many applications, which requires a satisfactory discrete implementation. Recently, hyperdifferential operators have been proposed as a novel way of defining the discrete LCT (DLCT). Here we first focus on improving the accuracy of this approach by considering alternative discrete coordinate multiplication and differentiation operations. We also consider canonical decompositions of LCTs and compare them with the originally proposed Iwasawa decomposition. We show that accuracy of the approximation of the continuous LCT with the DLCT can be drastically improved. The advantage and elegance of this approach lie in the fact that it reduces the problem of defining sophisticated discrete transforms to merely defining discrete coordinate multiplication and differentiation operations, by reducing the transforms to these operations. As a result of systematic investigation of possible parameters and design choices, we achieve a DLCT that is both theoretically satisfying and highly accurate.

1. Introduction

The family of linear canonical transforms (LCTs) generalizes several important transforms and operations such as the fractional Fourier transform (FRFT), chirp multiplication (CM), chirp convolution (CC), and scaling [1–5], which are special cases of the LCT [3]. Two-dimensional (2D) and complex-parametered extensions of LCTs have also been studied [6–9]. Other important transforms such as the gyrator transform, the bilateral Laplace transforms, the Bargmann transform, the Gauss-Weierstrass transform, the fractional Laplace transform, and complex-ordered FRFTs [1,10–18], are all special cases of complex and/or 2D-LCTs.

Sometimes referred by other names such as generalized Huygens integrals [19], generalized Fresnel transforms [20,21], special affine Fourier transforms [22,23], extended fractional Fourier transforms [24], and Moshinsky-Quesne transforms [1], the class of LCTs are important in signal processing [3], computational and applied mathematics [25,26], optics [27–29], and quantum mechanics [1,3,30–32]. Prominent signal processing applications include fast and efficient optimal filtering [33], radar signal processing [34,35], speech processing [36], and image representation, encryption and watermarking [37–40]. LCTs are known as quadratic-phase integrals or quadratic-phase systems [28,29] in optics and wave propagation applications and they have also been well studied in these contexts [2,19,28,41–44].

The deployment of LCTs in the aforementioned applications requires a concrete framework for discretization and development of digital computation methods. Methods for discretization and digital computation have been proposed [29,45–60]. These previous approaches either directly map the samples of the continuous input signal to the samples of the output signal by digitally computing the continuous integral, or first define a discrete LCT (DLCT) and then use it to approximate the continuous LCT (analogous to first defining the discrete Fourier transform (DFT) and then using it to approximate the continuous Fourier transform (FT)). Further review of the literature can be found in [3,26,61]. There are also works [56,57] that focus on developing efficient numerical computation algorithms based on a previously-defined DLCT. One of the most important special cases of LCTs is the FRFT, for which discrete definitions and digital computation methods are also present in the literature, [62–75].

Recently, hyperdifferential operators have been used to define the DLCT [61]. This definition uses discrete versions of the simple building blocks of coordinate multiplication, differentiation and the FT in a way that is totally consistent with the established definition of the DFT. The approach presented in [61] has emphasized the preservation of the general structural symmetry between coordinate multiplication and differentiation operations. That work emphasizes mathematical consistency and structural analogy with the continuous transform family, more than focusing on numerical accuracy. Accuracy increases with increasing number of sample

* Corresponding author at: Department of Electrical and Electronics Engineering, Bilkent University, Bilkent, Ankara, Turkey.
E-mail address: aykut.koc@bilkent.edu.tr (A. Koç).

https://doi.org/10.1016/j.sigpro.2021.108291
0165-1684/

points N, as with most transforms, but maximizing accuracy for a given value of N is not the focus of that paper. Since increasing N brings computational, transmission, and storage burdens, in this paper we examine alternatives to the straightforward numerical implementations of the basic buildings blocks in search of more accurate implementations, and show that significant improvements in accuracy are possible. Moreover, in [61], only the Iwasawa decomposition is considered in defining the hyperdifferential operator based DLCT. In this paper we also consider other decompositions and examine their effects on performance. Thus, we build on [61] in two ways:

(i) considering the use of Canonical Decompositions Type I and Type II and comparing them with the originally-proposed Iwasawa Decomposition,
(ii) proposing several alternative discrete coordinate multiplication and differentiation definitions to improve accuracy.

We report a large accuracy improvement for the operator theory-based DLCT by deploying alternative coordinate multiplication and differentiation definitions. Also, all major widely-used LCT decompositions are exhaustively compared. Thus, as a result of systematic investigation of possible parameters and design choices, we achieve a DLCT that is both theoretically satisfying and highly accurate. Another contribution of this paper is to demonstrate that the operator theory approach reduces the complicated problem of defining a DLCT to simply choosing the definition of fundamental operations such as discrete coordinate multiplication and discrete differentiation. This choice is the primary factor that determines the accuracy of the approach, whereas the choice of decomposition has relatively little effect.

The organization of the paper is as follows: Section 2 gives the preliminaries and the definition and important properties of LCTs. Section 3 describes the decompositions of LCTs. In Section 4, we review the hyperdifferential operator based approach to DLCT definition and present our proposed DLCT. In Section 5, numerical examples and comparisons are provided. Lastly, we conclude in Section 6.

2. Preliminaries

LCTs are unitary transforms specified by a 2×2 parameter matrix $\mathbf{L}=[A\ B;C\ D]$ with the constraint that the determinant of $\mathbf{L}$ is equal to 1 and A, B, C and D are all real. The definition of LCTs as linear integral transforms is given below:

$$\mathcal{C}_{\mathbf{L}}f(u)=\frac{1}{\sqrt{B}}\,e^{-i\pi/4}\int_{-\infty}^{\infty}\exp\left[i2\pi\left(\frac{D}{2B}u^2-\frac{1}{B}uu'+\frac{A}{2B}u'^2\right)\right]f(u')\,du', \tag{1}$$

where $\mathcal{C}_{\mathbf{L}}$ denotes the LCT operator and where the subscript $\mathbf{L}$ denotes the 2×2 parameter matrix.

The following operations are important special cases of LCTs. Scaling operation is defined by $\mathcal{C}_{\mathbf{L}_M}f(u)=\mathcal{M}_Mf(u)=\sqrt{1/M}\,f(u/M)$ and its parameter matrix is $\mathbf{L}_M=[M\ 0;0\ 1/M]$. The fractional Fourier transform (FRFT), as denoted by $\mathcal{F}^a$, is the generalization of the FT with the following definition [2]:

$$\mathcal{F}^af(u)=\int_{-\infty}^{\infty}A_\theta\exp\left[i\pi\left(u^2\cot\theta-2uu'\csc\theta+u'^2\cot\theta\right)\right]f(u')\,du',$$
$$A_\theta=\frac{\exp(-i\pi\,\mathrm{sgn}(\sin\theta)/4+i\theta/2)}{|\sin\theta|^{1/2}}. \tag{2}$$

The parameter matrix of FRFT is given by $\mathbf{L}_{\mathcal{F}^a_{\mathrm{lc}}}=[\cos\theta\ \ \sin\theta;-\sin\theta\ \ \cos\theta]$ where $\theta=\pi a/2$ and a is the fractional order. When $a=1$, the FRFT reduces to the FT. It should be noted that there is an inconsequential difference between $\mathcal{F}^a_{\mathrm{lc}}$ and the more commonly used definition $\mathcal{F}^a$ of the FRFT, [2]. Chirp multiplication (CM) is defined as $\mathcal{C}_{\mathbf{Q}_q}f(u)=\mathcal{Q}_qf(u)=\exp(-i\pi qu^2)f(u)$ with the following parameter matrix $\mathbf{L}_{\mathbf{Q}_q}=[1\ 0;-q\ \ 1]$. Chirp convolution (CC) is expressed by $\mathcal{C}_{\mathbf{R}_r}f(u)=\mathcal{R}_rf(u)=f(u)*e^{-\frac{\pi}{4}}\sqrt{1/r}\exp\left(i\pi u^2/r\right)$ with the parameter matrix $\mathbf{L}_{\mathbf{R}_r}=[1\ \ r;0\ \ 1]$.

3. Decompositions of LCTs

The LCT operator $\mathcal{C}_{\mathbf{L}}$ can be expressed as combinations of other simpler operators. Using scaling $\mathcal{M}_M$, chirp multiplication $\mathcal{Q}_q$, chirp convolution $\mathcal{R}_r$ and fractional Fourier $\mathcal{F}^a_{\mathrm{lc}}$ operators, we are able to construct any LCT. The decompositions utilized in this paper are

$$\mathcal{C}_{\mathbf{L}}=\mathcal{Q}_q\mathcal{M}_M\mathcal{F}^a_{\mathrm{lc}}, \tag{3}$$

$$\mathcal{C}_{\mathbf{L}}=\mathcal{R}_{r_2}\mathcal{Q}_q\mathcal{R}_{r_1}, \tag{4}$$

$$\mathcal{C}_{\mathbf{L}}=\mathcal{Q}_{q_2}\mathcal{R}_r\mathcal{Q}_{q_1}. \tag{5}$$

(3) is known as the Iwasawa decomposition. (4) and (5) are the CC-CM-CC and CM-CC-CM decompositions, also known as Canonical Decompositions Type I and Type II, respectively. a is the order of FRFT and q, r, and M are the parameters of chirp multiplication, chirp convolution, and scaling operations. How these parameters are determined is given below.

3.1. The iwasawa decomposition

Using scaling $\mathcal{M}_M$, chirp multiplication $\mathcal{Q}_q$ and fractional Fourier $\mathcal{F}^a_{\mathrm{lc}}$ operators, it is possible to construct any LCT operator $\mathcal{C}_{\mathbf{L}}$. The Iwasawa breaks down an arbitrary LCT into a FRFT followed by a scaling followed by a chirp multiplication. When each operator is characterized by their 2×2 LCT parameter matrix, the decomposition looks like

$$\mathbf{L}=\begin{bmatrix}A & B\\ C & D\end{bmatrix}=\begin{bmatrix}1 & 0\\ -q & 1\end{bmatrix}\begin{bmatrix}M & 0\\ 0 & 1/M\end{bmatrix}\begin{bmatrix}\cos a\pi/2 & \sin a\pi/2\\ -\sin a\pi/2 & \cos a\pi/2\end{bmatrix} \tag{6}$$

where $q=-(AC+BD)/(A^2+B^2)$, $M=\sqrt{A^2+B^2}$, and a must satisfy $\cos(a\pi/2)=A/M$ and $\sin(a\pi/2)=B/M$.

3.2. Canonical decomposition type I (CC-CM-CC)

Canonical decomposition Type I breaks down an arbitrary LCT into a chirp convolution followed by a chirp multiplication followed by a second chirp convolution. When each operator is characterized by their 2×2 LCT parameter matrix, the decomposition then looks like

$$\mathbf{L}=\begin{bmatrix}A & B\\ C & D\end{bmatrix}=\begin{bmatrix}1 & r_2\\ 0 & 1\end{bmatrix}\begin{bmatrix}1 & 0\\ -q & 1\end{bmatrix}\begin{bmatrix}1 & r_1\\ 0 & 1\end{bmatrix}. \tag{7}$$

The decomposition parameters are computed using the following equalities: $r_1=(D-1)/C$, $q=-C$ and $r_2=(A-1)/C$.

3.3. Canonical decomposition type II (CM-CC-CM)

Being the dual of Type I, Canonical decomposition Type II breaks down an arbitrary LCT into a chirp multiplication followed by a chirp convolution followed by a second chirp multiplication. When each operator is characterized by their 2×2 LCT parameter matrix, the decomposition then looks like

$$\mathbf{L}=\begin{bmatrix}A & B\\ C & D\end{bmatrix}=\begin{bmatrix}1 & 0\\ -q_2 & 1\end{bmatrix}\begin{bmatrix}1 & r\\ 0 & 1\end{bmatrix}\begin{bmatrix}1 & 0\\ -q_1 & 1\end{bmatrix}, \tag{8}$$

where the decomposition parameters are $q_1=(1-A)/B$, $r=B$ and $q_2=(1-D)/B$.

4. The discrete linear canonical transforms

In [61], hyperdifferential operators and the Iwasawa decomposition have been used to define a DLCT. Building upon this framework, we propose to use other decompositions to define improved hyperdifferential operator based DLCT variants. The general approach is to decompose LCTs into simpler building blocks, find discrete versions of these blocks by using operator theory, and then multiply them to obtain the final DLCT matrix. We start with presenting the hyperdifferential forms of the simple building blocks.

4.1. The hyperdifferential forms

The term hyperdifferential refers to having differential operators in an exponent. In the LCT context, we only have second order coordinate multiplication and differentiation operators in the exponent. Operators representing an arbitrary LCT or all of its special cases can be generated by exponentiating these second order operators and these constitute the hyperdifferential forms of these transforms. There is correspondence among the integral transforms, hyperdifferential operators and the 2×2 parameter matrices that are given in the preliminaries section. An LCT can be represented by any one of these mathematical objects [61]. More details can be found in [1].

Chirp multiplication operator $\mathcal{Q}_q$, chirp convolution operator $\mathcal{R}_r$, scaling operator $\mathcal{M}_M$, and fractional Fourier transform operator $\mathcal{F}^a_{\text{lc}}$ can all be written in hyperdifferential forms as follows: [1,2]:

$$\mathcal{Q}_q = \exp\left(-i2\pi q\frac{\mathcal{U}^2}{2}\right), \tag{9}$$

$$\mathcal{R}_r = \exp\left(-i2\pi r\frac{\mathcal{D}^2}{2}\right), \tag{10}$$

$$\mathcal{M}_M = \exp\left(-i2\pi \ln(M)\frac{\mathcal{U}\mathcal{D}+\mathcal{D}\mathcal{U}}{2}\right), \tag{11}$$

$$\mathcal{F}^a_{\text{lc}} = \exp\left(-ia\pi^2\frac{\mathcal{U}^2+\mathcal{D}^2}{2}\right), \tag{12}$$

where $\mathcal{U}$ and $\mathcal{D}$ are the coordinate multiplication and differentiation operators, respectively. We see that all three of the operators we are working with can be expressed in terms of these two building blocks, whose continuous manifestations are:

$$\mathcal{U}f(u) = uf(u) \tag{13}$$

$$\mathcal{D}f(u) = \frac{1}{i2\pi}\frac{df(u)}{du}, \tag{14}$$

where the $(i2\pi)^{-1}$ is included so that $\mathcal{U}$ and $\mathcal{D}$ are precisely Fourier duals (the effect of either in one domain is its dual in the Fourier domain). This duality can be expressed as follows:

$$\mathcal{U} = \mathcal{F}\mathcal{D}\mathcal{F}^{-1}. \tag{15}$$

4.2. The discrete linear canonical transform definitions based on decompositions

Our approach is based on requiring that, to the extent possible, all the discrete entities we define observe the same structural relationships as they do in abstract operator form. We want a discrete definition that is as analogous to the continuous definition as possible. To ensure this, we define the DLCT and its special cases as the discrete manifestations of the decompositions Eqs. (3)–(5) with the abstract operators being replaced by matrix operators. This can be written as follows:

$$\mathbf{C_L} = \mathbf{Q}_q\mathbf{M}_M\mathbf{F}^a_{\text{lc}}, \tag{16}$$

$$\mathbf{C_L} = \mathbf{R}_{r_2}\mathbf{Q}_q\mathbf{R}_{r_1}, \tag{17}$$

$$\mathbf{C_L} = \mathbf{Q}_{q_2}\mathbf{R}_r\mathbf{Q}_{q_1}. \tag{18}$$

Similarly, the special cases can also be written in matrix form as

$$\mathbf{Q}_q = \exp\left(-i2\pi q\frac{\mathbf{U}^2}{2}\right), \tag{19}$$

$$\mathbf{R}_r = \exp\left(-i2\pi r\frac{\mathbf{D}^2}{2}\right), \tag{20}$$

$$\mathbf{M}_M = \exp\left(-i2\pi \ln(M)\frac{\mathbf{UD}+\mathbf{DU}}{2}\right), \tag{21}$$

$$\mathbf{F}^a_{\text{lc}} = \exp\left(-ia\pi^2\frac{\mathbf{U}^2+\mathbf{D}^2}{2}\right), \tag{22}$$

where exp() in the above equations denote matrix exponentials. By substituting Eqs. (19)–(22) into Eqs. (16)–(18), one can write three different DLCT matrices as:

$$\mathbf{C_L} = \exp\left(-i2\pi q\frac{\mathbf{U}^2}{2}\right)\times \exp\left(-i2\pi \ln(M)\frac{\mathbf{UD}+\mathbf{DU}}{2}\right)\exp\left(-ia\pi^2\frac{\mathbf{U}^2+\mathbf{D}^2}{2}\right), \tag{23}$$

$$\mathbf{C_L} = \exp\left(-i2\pi r_2\frac{\mathbf{D}^2}{2}\right)\exp\left(-i2\pi q\frac{\mathbf{U}^2}{2}\right)\exp\left(-i2\pi r_1\frac{\mathbf{D}^2}{2}\right), \tag{24}$$

$$\mathbf{C_L} = \exp\left(-i2\pi q_2\frac{\mathbf{U}^2}{2}\right)\exp\left(-i2\pi r\frac{\mathbf{D}^2}{2}\right)\exp\left(-i2\pi q_1\frac{\mathbf{U}^2}{2}\right). \tag{25}$$

To obtain the DLCT of a function of a discrete variable, we just need to write it as a column vector and then multiply it with the DLCT matrix. In mathematical terms, the LCT of a signal $\mathbf{x} = [x[1], x[2], \ldots, x[n]]^T$ of length N is given by $\mathbf{C_L x}$, yielding an $N\times 1$ output. Since $\mathbf{C_L}$ is an $N\times N$ matrix, the operation does not change the number of samples of the input signal.

At this point, the only ingredients missing are the matrices corresponding to each elementary operator. The proposed DLCT matrices will be defined as the matrix product of three of the following matrices: FRFT, scaling, and chirp multiplication or convolution, all of which are defined in terms of only two matrices: **U** and **D**. Therefore, it is seen that all rest on the definition of the differentiation and coordinate multiplication matrices **D** and **U**. The operator based framework reduces the task of defining a DLCT into defining discrete forms of the relatively basic operations of coordinate multiplication and differentiation. Actually, since as a consequence of the duality relation these two simple operations can be obtained from one another, it is actually necessary to only define one of them, upon which the other will have been automatically defined. Once we choose the definition of **U** (or **D**), everything else is handled by the requirement of maintaining structural analogy with the continuous definition. Of course, with so much resting on the definition of **U** and **D**, making the right choice becomes more critical. Making the best choice possible is the purpose of this paper. So, we move to elaborate on procedures to obtain the **U** and **D** matrices.

4.3. Alternative definitions of **U** and **D** matrices

4.3.1. Structurally analogous **U** and **D** matrices

The first alternative we consider is the theoretically derived **U** and **D** matrices that were originally proposed in [61]. The theoretical derivation begins with the definition of finite differencing as an approximation to the derivative of a continuous function. By using operator theory, the finite difference operation is derived as a function of the continuous $\mathcal{D}$ operator. Then, to preserve structural symmetry between the two domains, the discrete version of the coordinate multiplication operator is also written in terms of the continuous $\mathcal{U}$ operator exactly in the same functional form as for finite differencing. Finally, the dualiy relation can be used to relate these two main building blocks. Further details are given in [61]. The result is the following matrix elements for **U**:

$$U_{mn} = \begin{cases} \frac{\sqrt{N}}{\pi} \sin\left(\frac{\pi}{N} n\right), & \text{for } m = n \\ 0, & \text{for } m \neq n \end{cases}, \tag{26}$$

where $m, n = 0, 1, \ldots, N-1$ and N is the number of samples. The discrete version of the duality relation given in Eq. (15) can be used to define the matrix **D** in terms of **U** by using

$$\mathbf{D} = \mathbf{F}^{-1}\mathbf{U}\mathbf{F}, \tag{27}$$

in which **F** is the matrix representing the N-point unitary discrete Fourier transform, with elements F_{mn} being $W_N = \exp(-j2\pi/N)$ as $F_{mn} = \frac{1}{\sqrt{N}} W_N^{mn}$.

4.3.2. Formally analogous **U** and **D** matrices

Here we consider the most straightforward and formal way of discretizing the continuous coordinate multiplication operator to obtain **U** matrix. We simply form a diagonal matrix with the diagonal entries being equal to the coordinate values, in order to mimic the appearance of the continuous case. Let us have N samples and sample over an extent $\sqrt{N}$ with sampling interval $h = 1/\sqrt{N}$. Then, $\mathcal{U}f(u) = uf(u)$ can be discretized as $nhf(nh) = n/\sqrt{N} f[n]$ where $u = nh$ and $n = 0, 1, \ldots, N-1$. So we have

$$U_{mn} = \begin{cases} \frac{n}{\sqrt{N}}, & \text{for } m = n \\ 0, & \text{for } m \neq n \end{cases}, \tag{28}$$

where $m, n = 0, 1, \ldots, N-1$. It is also interesting to observe that this corresponds to the limit of Eq. (26) as $N \to \infty$. Again, since we want **U** and **D** to be Fourier duals of each other in order to preserve the dual structure of the definition, we use the discrete version of the duality relation given in Eq. (27) to obtain **D** matrix.

4.3.3. Numerical analysis inspired **U** and **D** matrices

The third alternative we will study is highly accurate numerical forms of **U** and **D** from the numerical computation literature (specifically, spectral methods [76], that are advanced numerical techniques from scientific computing primarily used for numerically solving differential equations).

Different from the first two approaches where we first defined **U** and then obtained **D** from the duality, here we start with first defining discrete differentiation and then using the duality relation to obtain discrete coordinate multiplication.

We use the discrete first-order differentiation matrix **D** from [76]. This matrix is obtained using spectral methods and defined for even N as:

$$\mathbf{D}_{mn} = \begin{cases} 0, & \text{for } m = n \\ \frac{1}{2}(-1)^{m-n} \cot\left(\frac{(m-n)\pi}{N}\right), & \text{for } m \neq n \end{cases} \tag{29}$$

where $m, n = 0, \ldots, N-1$. Also, note that a version of the above definition for odd N also exists but, for simplicity, we keep our framework for the case of even N, which is usually the case. If needed, extension to the odd N case is also possible.

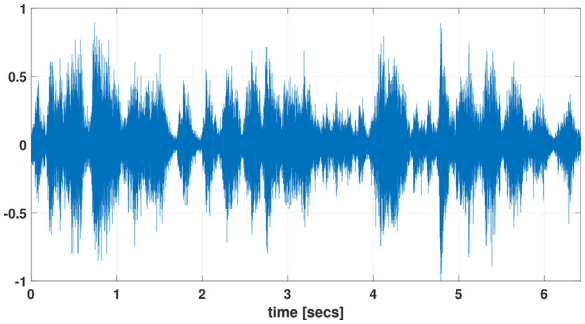

Fig. 1. Example vocal signal 'laughter.wav'. Sampling rate: 8192 Hz.

Then, by using the duality relation ($\mathbf{U} = \mathbf{F}\mathbf{D}\mathbf{F}^{-1}$), one can easily obtain the discrete coordinate multiplication matrix **U**. By replacing the numerically obtained **U** and **D** matrices in Eqs. (23)–(25), we reach versions of the proposed DLCT definitions for all of the three decomposition cases.

To sum up, for each of three decompositions with each of three **U** and **D** matrix pairs, we present a total of nine variations for finding the DLCT matrix.

5. Numerical results and comparisons

5.1. Input functions and transforms

In this section, we numerically explore how well the DLCT definitions obtained by combinations of the presented decompositions and alternative **U** and **D** definitions, approximates the continuous LCT. Recall that we have three methods of defining **U** and **D** matrices: (1) Structurally analogous matrices (called "Structural"); (2) Formally analogous matrices as defined the limits of Case 1 (called "Formal"); (3) Numerical analysis inspired matrices (called "Numerical"). We also consider three different decompositions used: Iwasawa, Canonical Decompositions Type I and Type II (called "Type I" and "Type II", respectively). We carried out extensive experiments for all combinations of these two sets of alternatives. Moreover, we also performed experiments with the method in [49], which is a digital numerical computation algorithm which provides an accurate approximation in $O(N \log N)$ time.

We consider the following example input functions: the chirped pulse function $\exp(-\pi u^2 - i\pi u^2)$, denoted by F1, the trapezoidal function $1.5\mathrm{tri}(u/3) - 0.5\mathrm{tri}(u)$, denoted by F2 ($\mathrm{tri}(u) = \mathrm{rect}(u) * \mathrm{rect}(u)$), the damped sine function $\exp(-2|u|)\sin(3\pi u)$, denoted by F3, and the binary sequence 01101010 adjusted for the number of samples N, denoted by F4, are used.

We also considered a non-synthetic vocal signal, 'laughter.wav', which is one of MATLAB's built-in audio signals. Plotted in Fig. 1, 'laughter' is a vocal signal sampled with a rate of 8.192 kHz. With 52,634 samples, it has a total duration of 6.425 s.

We performed experiments with six transforms, denoted by T1, T2, T3, T4, T5, and T6, with parameters $(\alpha, \beta, \gamma) = (-3, -2, -1)$, $(2.1, -1.7, 0.02)$, $(-0.8, 3, 1)$, $(0.6, 1.1, -0.4)$, $(-1.8, -1.75, -1.3)$, $(-2.5, 3, 0.1)$, respectively. As a reference, we employed a highly inefficient brute force numerical approach and calculated mean squared errors (MSEs) of the proposed DLCT outputs as well as the baseline method in [49] with respect to this reference for F1 to F4. Since the baseline method is not a definition for the discrete LCT, but rather an algorithm for digital numerical computation, it may modify the sampling structure. To ensure fair and controlled comparisons, results of the baseline method are interpolated such that the coordinate structure of the samples are aligned with the reference. Since 'laughter' is a real signal, it does not have an analytical expression that can be used to calculate a reference that will

Table 1
Percentage MSE errors for function F2 (TRAPEZOID) and transform T1 for different decompositions and DLCT methods, and method from Koç et al. [49].

Method	N	Iwasawa	Type I	Type II
Structural	256	4.31	3.14	1.21×10^{1}
	512	1.20	1.04	4.30
	1024	3.15×10^{-1}	3.23×10^{-1}	1.29
Formal	256	9.87×10^{-5}	6.88×10^{-5}	6.88×10^{-5}
	512	1.08×10^{-5}	8.04×10^{-6}	8.04×10^{-6}
	1024	6.16×10^{-6}	5.17×10^{-6}	5.17×10^{-6}
Numerical	256	9.75×10^{-5}	6.88×10^{-5}	6.88×10^{-5}
	512	1.05×10^{-5}	8.04×10^{-6}	8.04×10^{-6}
	1024	5.91×10^{-6}	5.17×10^{-6}	5.17×10^{-6}
	N	Digital Numerical Computation		
Method from Koç et al. [49]	256	4.88×10^{-5}		
	512	7.50×10^{-6}		
	1024	3.90×10^{-6}		

Table 2
Percentage MSE errors for function F2 (TRAPEZOID) and transform T3 for different decompositions and DLCT methods, and method from Koç et al. [49].

Method	N	Iwasawa	Type I	Type II
Structural	256	1.06×10^{1}	9.71×10^{1}	5.61×10^{1}
	512	3.24	8.05×10^{1}	3.62×10^{1}
	1024	8.68×10^{-1}	5.95×10^{1}	1.83×10^{1}
Formal	256	4.21×10^{-4}	8.96×10^{-1}	6.68×10^{-4}
	512	3.79×10^{-5}	2.06×10^{-5}	1.99×10^{-5}
	1024	1.58×10^{-5}	4.82×10^{-6}	6.45×10^{-6}
Numerical	256	4.06×10^{-4}	1.12	7.67×10^{-4}
	512	4.07×10^{-5}	2.07×10^{-5}	2.19×10^{-5}
	1024	1.38×10^{-5}	4.82×10^{-6}	6.46×10^{-6}
	N	Digital Numerical Computation		
Method from Koç et al. [49]	256	1.44×10^{-3}		
	512	3.43×10^{-5}		
	1024	5.71×10^{-6}		

serve as a basis for comparison. Thus, we performed three consecutive LCT transformations such that the third one is the inverse of the concatenation of the former two. Since the overall operation is an identity, the result of applying these three transforms should ideally be equal to the original input signal. Therefore, the accuracy performance in this case has been calculated by comparing the actual output to the original input signal. These experiments have the additional benefit of providing confirmation of the additivity/reversibility properties of the proposed DLCT. Moreover, this experiment also tests the additivity/reversibility properties of the proposed DLCT. The performance metric is defined as the energy of the difference normalized by the energy of the reference, expressed as a percentage. The number of samples N are taken as 256, 512, and 1024 for three sets of numerical simulations. Since 'laughter' is a signal of 52,634 samples with quite high frequency components, it is not possible to compute a DLCT of size 52,634 as a single transform. Therefore, experiments were performed as follows: we start with the first 64 samples and zero-pad to form signals of length 256, 512 and 1024. We calculate the LCT and then move 1 sample to the right to form another signal. We continue in this manner until we finish the entire sequence of 52,634. This produces 52,571 chunks of input and we report average accuracy values coming from 52,571 runs.

5.2. Numerical results

The resulting percentage MSE scores for F2-T1, F2-T3, F3-T2 and F3-T4 are tabulated in Tables 1–4. Upon inspecting these results, it

Table 3
Percentage MSE errors for function F3 (DAMPED SINE) and transform T2 for different decompositions and DLCT methods, and method from Koç et al. [49].

Method	N	Iwasawa	Type I	Type II
Structural	256	1.78×10^{1}	1.43×10^{2}	1.89×10^{1}
	512	4.87	9.03×10^{1}	7.52
	1024	1.28	3.85×10^{1}	2.74
Formal	256	3.48×10^{-4}	1.54×10^{-3}	3.32×10^{-4}
	512	4.86×10^{-5}	2.04×10^{-4}	4.83×10^{-5}
	1024	7.00×10^{-6}	2.91×10^{-5}	6.99×10^{-6}
Numerical	256	3.48×10^{-4}	1.54×10^{-3}	3.32×10^{-4}
	512	4.86×10^{-5}	2.04×10^{-4}	4.83×10^{-5}
	1024	7.00×10^{-6}	2.91×10^{-5}	6.99×10^{-6}
	N	Digital Numerical Computation		
Method from [49]	256	4.94×10^{-4}		
	512	6.94×10^{-5}		
	1024	1.00×10^{-5}		

Table 4
Percentage MSE errors for function F3 (DAMPED SINE) and transform T4 for different decompositions and DLCT methods, and method from Koç et al. [49].

Method	N	Iwasawa	Type I	Type II
Structural	256	5.76	6.80	3.47×10^{1}
	512	1.56	2.10	1.41×10^{1}
	1024	4.18×10^{-1}	5.56×10^{-1}	4.89
Formal	256	3.64×10^{-4}	3.62×10^{-4}	3.54×10^{-4}
	512	5.08×10^{-5}	5.07×10^{-5}	5.04×10^{-5}
	1024	7.33×10^{-6}	7.32×10^{-6}	7.31×10^{-6}
Numerical	256	3.64×10^{-4}	3.62×10^{-4}	3.54×10^{-4}
	512	5.08×10^{-5}	5.07×10^{-5}	5.04×10^{-5}
	1024	7.32×10^{-6}	7.32×10^{-6}	7.31×10^{-6}
	N	Digital Numerical Computation		
Method from [49]	256	3.66×10^{-4}		
	512	5.13×10^{-5}		
	1024	7.40×10^{-6}		

Table 5
Percentage MSE errors for function F1 (CHIRPED PULSE) and transform T5 for different decompositions and DLCT methods, and method from Koç et al. [49].

Method	N	Iwasawa	Type I	Type II
Formal	256	5.40×10^{-22}	5.42×10^{-22}	5.45×10^{-22}
	512	5.39×10^{-22}	5.47×10^{-22}	5.40×10^{-22}
	1024	5.65×10^{-22}	5.52×10^{-22}	5.53×10^{-22}
Numerical	256	5.45×10^{-22}	5.43×10^{-22}	5.42×10^{-22}
	512	5.46×10^{-22}	5.57×10^{-22}	5.40×10^{-22}
	1024	5.44×10^{-22}	5.32×10^{-22}	5.37×10^{-22}
	N	Digital Numerical Computation		
Method from Koç et al. [49]	256	1.49×10^{-9}		
	512	1.01×10^{-10}		
	1024	6.42×10^{-12}		

can be seen that the proposed DLCT that uses "Formal" and "Numerical" **U** and **D** matrices, overwhelmingly outperforms the DLCT with "Structural" definition of these building blocks. The same observation is also present in other experiments we performed and cannot present here due to length constraints. Given the clear numerical inferiority of "Structural" approach, in our further examples we eliminate it from consideration and provide further results only for the "Formal" and "Numerical" alternatives. In Tables 5 and 6, we present results for F1-T5 and F4-T5. Some examples from our results are also plotted in Fig. 2.

We consider the transform concatenations T5-T6, T4-T2, T1-T3 and T1-T5 on the 'laughter' signal such that $\mathbf{C}_{L_5L_6}^{-1}\mathbf{C}_{L_5}\mathbf{C}_{L_6}$ is equal to the identity operation. The MSE scores of recovered signals and

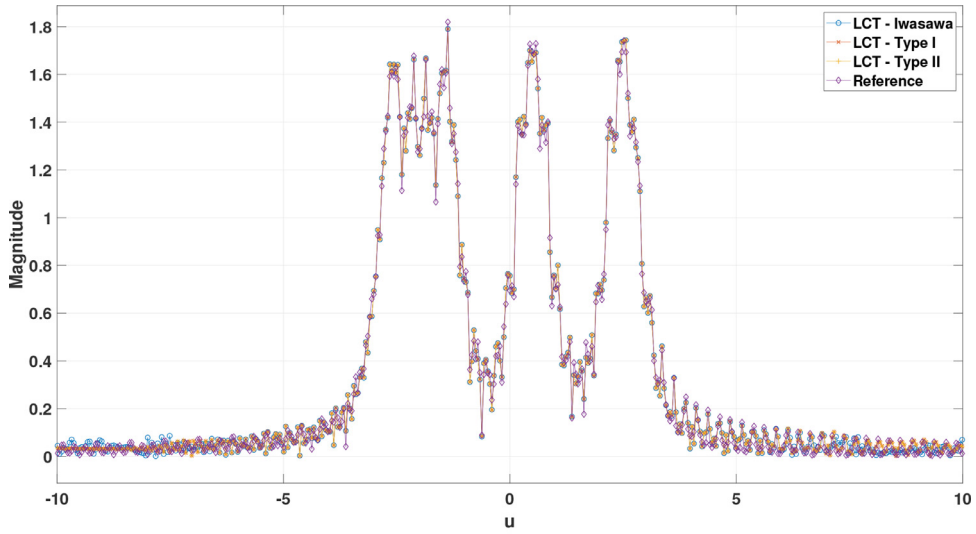

(a) Magnitude of T1 of F4

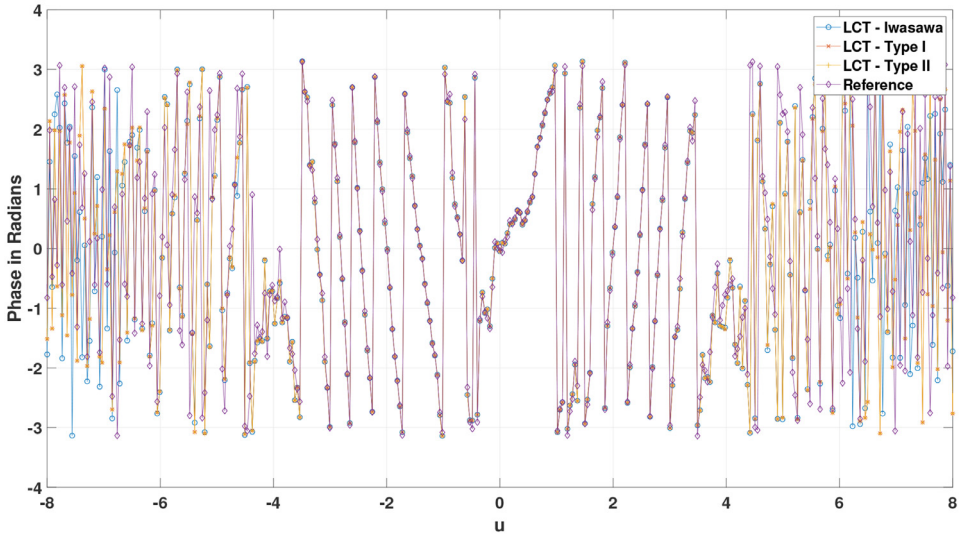

(b) Phase of T1 of F4

Fig. 2. Magnitude and phase of T1 of F4 (Binary) for "Formal" DLCT method and different decompositions.

Table 6
Percentage MSE errors for function F4 (BINARY) and transform T5 for different decompositions and DLCT methods, and method from Koç et al. [49].

Method	N	Iwasawa	Type I	Type II
Formal	256	1.34	1.28	1.31
	512	3.46×10^{-1}	3.68×10^{-1}	3.40×10^{-1}
	1024	4.59×10^{-1}	4.56×10^{-1}	4.57×10^{-1}
Numerical	256	1.30	1.28	1.32
	512	3.48×10^{-1}	3.73×10^{-1}	3.40×10^{-1}
	1024	4.61×10^{-1}	4.55×10^{-1}	4.58×10^{-1}
	N	Digital Numerical Computation		
Method from [49]	256		1.19	
	512		3.15×10^{-1}	
	1024		4.34×10^{-1}	

inputs are tabulated in Tables 9–12 for different N values, decompositions, DLCT methods and the digital numerical computation based method.

5.3. Additional notes

Upon inspecting the results presented in Tables 1–6, it is clear that the "Formal" and "Numerical" methods are almost equivalent in terms of accuracy, considering the inconsequential differences between their respective MSE scores. Since these two methods give almost identical results, from now on we will focus on "Formal" approach, which is the simpler of the two. In Tables 7 and 8, we present results for several additional combinations of functions and transforms, specifically for "Formal" approach.

Another observation is that the effect of the decomposition used is minimal. In general, none of the Iwasawa, Type I and Type II decompositions can present a decisive advantage upon others, and whichever is most preferable based on other considerations can be preferred.

Note that we are considering three alternative definitions for **U** and **D** matrices, three decompositions, four functions, and six transforms, as well as three different values of N. This leads to 648

Table 7
Percentage MSE errors for function F1 (CHIRPED PULSE) and transforms T2, T3, T6 FOR "FORMAL" DLCT method and different decompositions, and method from Koç et al. [49].

Transform	N	Iwasawa	Type I	Type II	Method from [49]
T2	256	5.40×10^{-22}	1.50×10^{-17}	5.37×10^{-22}	1.17×10^{-7}
	512	5.34×10^{-22}	5.48×10^{-22}	5.50×10^{-22}	6.85×10^{-9}
	1024	5.69×10^{-22}	5.29×10^{-22}	5.40×10^{-22}	4.01×10^{-10}
T3	256	2.44×10^{-15}	1.71×10^{-19}	1.29×10^{-17}	1.04×10^{-8}
	512	5.47×10^{-22}	5.49×10^{-22}	5.44×10^{-22}	8.29×10^{-10}
	1024	5.24×10^{-22}	5.42×10^{-22}	5.36×10^{-22}	2.93×10^{-11}
T6	256	5.51×10^{-16}	5.45×10^{-22}	9.51×10^{-11}	1.12×10^{-12}
	512	5.30×10^{-22}	5.45×10^{-22}	1.48×10^{-21}	1.81×10^{-13}
	1024	5.50×10^{-22}	5.54×10^{-22}	5.41×10^{-22}	3.14×10^{-14}

Table 8
Percentage MSE errors for function F4 (BINARY) and transforms T1, T4, T6 for "FORMAL" DLCT method and different decompositions, and method from Koç et al. [49].

Transform	N	Iwasawa	Type I	Type II	Method from Koç et al. [49]
T1	256	1.39	1.41	1.41	1.44
	512	4.18×10^{-1}	3.68×10^{-1}	3.68×10^{-1}	3.24×10^{-1}
	1024	5.06×10^{-1}	5.07×10^{-1}	5.07×10^{-1}	5.12×10^{-1}
T4	256	8.57×10^{-1}	2.25	2.48×10^{1}	9.06
	512	2.16×10^{-1}	2.30×10^{-1}	3.73×10^{-1}	2.29×10^{-1}
	1024	2.66×10^{-1}	2.66×10^{-1}	3.15×10^{-1}	2.57×10^{-1}
T6	256	7.48×10^{1}	1.08×10^{2}	1.03×10^{2}	5.48×10^{-1}
	512	5.14×10^{1}	7.45×10^{1}	6.74×10^{1}	1.25×10^{-1}
	1024	1.21×10^{1}	1.81×10^{1}	1.05×10^{1}	1.61×10^{-1}

Table 9
Percentage MSE Errors for vocal signal 'LAUGHTER' and transform pair T5-T6 for different decompositions and DLCT methods, and method from Koç et al. [49].

Method	N	Iwasawa	Type I	Type II
Structural	256	118.14	98.45	143.29
	512	124.66	77.75	131.16
	1024	129.59	91.74	127.81
Formal	256	15.86	6.01	11.39
	512	1.51	0.42	1.41
	1024	0.43	1.8×10^{-2}	0.43
Numerical	256	16.44	6.20	11.81
	512	1.5	0.42	1.43
	1024	0.42	1.9×10^{-2}	0.43
	N	Digital Numerical Computation		
Method from Koç et al. [49]	256	5.97		
	512	9.30×10^{-1}		
	1024	5.62×10^{-1}		

Table 10
Percentage MSE errors for vocal signal 'LAUGHTER' and transform pair T4-T2 for different decompositions and DLCT methods, and method from Koç et al. [49].

Method	N	Iwasawa	Type I	Type II
Structural	256	116.32	136.26	138.15
	512	117.04	153.86	138.99
	1024	114.95	143.66	131.12
Formal	256	3.89	3.33	2.99
	512	2.43	2.20	0.76
	1024	2.16	2.03	0.16
Numerical	256	4.02	3.53	3.04
	512	2.54	2.24	0.77
	1024	2.18	2.06	0.16
	N	Digital Numerical Computation		
Method from Koç et al. [49]	256	2.32		
	512	1.32		
	1024	1.18		

Table 11
Percentage MSE errors for vocal signaL 'LAUGHTER' and transform pair T1-T3 for different decompositions and DLCT methods, and method from Koç et al. [49].

Method	N	Iwasawa	Type I	Type II
Structural	256	123.16	143.75	153.49
	512	114.05	122.86	139.84
	1024	105.88	103.93	138.07
Formal	256	85.66	39.94	8.60
	512	39.82	4.8×10^{-3}	1.88
	1024	7.29	0.8×10^{-3}	0.56
Numerical	256	84.33	41.65	8.82
	512	39.68	9.5×10^{-3}	1.9
	1024	7.26	3.2×10^{-3}	0.56
	N	Digital Numerical Computation		
Method from Koç et al. [49]	256	32.99		
	512	4.83×10^{-3}		
	1024	5.26×10^{-4}		

Table 12
Percentage MSE errors for vocal signal 'LAUGHTER' and transform pair T1-T5 for different decompositions and DLCT methods, and method from [49].

Method	N	Iwasawa	Type I	Type II
Structural	256	126.96	52.87	97.22
	512	116.74	52.16	98.57
	1024	112.15	80.49	119.92
Formal	256	3.90	1.93	0.37
	512	3.26	1.50	9.14×10^{-2}
	1024	3.15	1.44	2.63×10^{-2}
Numerical	256	3.86	1.94	0.44
	512	3.43	1.50	0.10
	1024	3.28	1.45	2.63×10^{-2}
	N	Digital Numerical Computation		
Method from Koç et al. [49]	256	4.50		
	512	4.34		
	1024	4.29		

cases. However, examination of the results (both shown and not shown) allowed us to eliminate one of the definitions of **U** and **D** matrices, and show that the other two gave similar results. We also noted that all decompositions gave similar results. This allows us to focus on the effect of varying the remaining parameters, for which we presented half the possible combinations. Thus through systematic elimination, we have covered the parameter space in a sufficiently representative manner.

We now turn our attention to how the function and transform parameters affect the results. Although there are exceptions, we can observe that, for a given function, different transform parameters usually do not give considerably different results. A very important determinant of the final MSE is the time- or space-bandwidth product of the function and how N is chosen in relation to that product. Some of the functions have higher time-bandwidth products and naturally require a larger value of N to achieve a comparable error to functions with lower time-bandwidth product. The value of N chosen is closely related to truncation of the extent of the function in both the time and frequency domains, and the MSE is closely aligned with the energy in the truncated parts, [49]. It is observed in Tables 1 to 8 that, despite not being with high margins, the Iwasawa decomposition performs better than Type I and II decompositions for F4 (Binary) signal, which contains high frequencies. In the low- and mid-frequency range (input functions F2 and F3), Type I and II yield higher performances.

On the other hand, if we turn our attention to the real vocal signal example, we observe that there are LCT parameters where the Type I and II decompositions perform better than the Iwasawa case for the non-synthetic vocal signal with high frequency fluctuations. In this case, the performance of the "Structural" DLCT variant is even worse. Therefore, the proposed "Formal" and "Numerical" variants with the Type I and Type II decompositions are better options.

5.4. Computational considerations

All variants of the proposed DLCT operate through matrix multiplication and have complexity $O(N^2)$. There are several highly accurate fast $O(N \log N)$ computational methods for calculating the DLCT [49,53,54,56]. For example, we showed in [49], that we could digitally compute the continuous LCT to an accuracy limited by the uncertainty relationship, with a fast $O(N \log N)$ algorithm. However, these numerical computation methods do not exhibit the structural and operational properties we expect from a discrete transform definition. The DLCT definitions that are the subject of this paper are compatible with the discrete Fourier transform (DFT) and its circulant structure, and is highly desirable from an analytical and theoretical standpoint. An ultimate goal would be to find a fast algorithm for directly computing it, rather than numerically approximating it.

6. Conclusion

We studied the operator theory approach to discrete linear canonical transforms by exhaustively considering several possible parameters and design choices. We showed that a numerically superior DLCT can be obtained by making certain choices regarding the discrete coordinate multiplication and differentiation matrices. The formally analogous definition, which is the simplest definition, was comparable to the definition from numerical analysis and clearly superior to the structurally analogous definition. We also considered Type I and Type II Canonical Decompositions and compared them with the originally proposed Iwasawa decomposition. We conclude that the choice of decomposition had very little effect.

In [49], we had presented a fast ($O(N \log N)$ digital numerical computation method to compute the continuous LCT to the best accuracy permitted by the uncertainty relationship. The downside was that this method is not a discrete definition but merely a numerical computation method. Recently, in [61], we introduced an operator based DLCT with desired discrete transform properties. However, this DLCT, in its original form, does not provide very high accuracy. By employing several alternative discrete differentiation and coordinate multiplication definitions, as well as alternative decompositions, we identified a DLCT definition with very high accuracy, mostly on par with numerical approaches. Straightforward application of the definition proposed involves a matrix multiplication with complexity $O(N^2)$. Developing a fast algorithm for the proposed operator theory-based DLCT would save us from having to fall back from using a theoretically desirable definition to numerical approaches, when fast computation is required. This would bring together all desirable qualities in a single DLCT definition.

Declaration of Competing Interest

The authors declare that they have no known competing financial interests or personal relationships that could have appeared to influence the work reported in this paper.

CRediT authorship contribution statement

Aykut Koç: Conceptualization, Methodology, Software, Validation, Formal analysis, Investigation, Resources, Data curation, Visualization, Writing – original draft, Writing – review & editing. **Haldun M. Ozaktas:** Methodology, Formal analysis, Writing – original draft, Writing – review & editing.

Acknowledgment

H. M. Ozaktas acknowledges partial support of the Turkish Academy of Sciences.

References

[1] K.B. Wolf, Integral Transforms in Science and Engineering (Chapter 9: Construction and Properties of Canonical Transforms), Plenum Press, New York, 1979.
[2] H.M. Ozaktas, Z. Zalevsky, M.A. Kutay, The Fractional Fourier Transform with Applications in Optics and Signal Processing, Wiley, New York, 2001.
[3] J.J. Healy, M.A. Kutay, H.M. Ozaktas, e. J. T. Sheridan, Linear canonical transforms: Theory and applications, Springer, New York, NY, 2016.
[4] S.C. Pei, J.J. Ding, Eigenfunction of linear canonical transform, IEEE Trans. Signal Process. 50 (2002) 11–26.
[5] A. Koç, B. Bartan, H.M. Ozaktas, Discrete scaling based on operator theory, Digit. Signal Process. 108 (2021) 102904.
[6] J. Rodrigo, T. Alieva, M.L. Calvo, Optical system design for orthosymplectic transformations in phase space, J. Opt. Soc. Am. A 23 (2006) 2494–2500.
[7] A. Koç, H.M. Ozaktas, L. Hesselink, Fast and accurate computation of two-dimensional non-separable quadratic-phase integrals, J. Opt. Soc. Am. A 27 (6) (2010) 1288–1302.
[8] A. Koç, H.M. Ozaktas, L. Hesselink, Fast and accurate algorithm for the computation of complex linear canonical transforms, J. Opt. Soc. Am. A 27 (9) (2010) 1896–1908.
[9] Q. Feng, B.-Z. Li, Convolution and correlation theorems for the two-dimensional linear canonical transform and its applications, IET Signal Proc. 10 (2016) 125–132.
[10] L. Zhang, D. Wei, Image watermarking based on matrix decomposition and gyrator transform in invariant integer wavelet domain, Signal Process. 169 (2020) 107421.
[11] C.C. Shih, Optical interpretation of a complex-order Fourier transform, Opt. Lett. 20 (10) (1995) 1178–1180.
[12] L.M. Bernardo, O.D.D. Soares, Optical fractional Fourier transforms with complex orders, Appl. Opt. 35 (17) (1996) 3163–3166.
[13] C. Wang, B. Lu, Implementation of complex-order Fourier transforms in complex ABCD optical systems, Opt. Commun. 203 (1–2) (2002) 61–66.
[14] L.M. Bernardo, Talbot self-imaging in fractional Fourier planes of real and complex orders, Opt. Commun. 140 (1997) 195–198.
[15] K.B. Wolf, Canonical transformations i. complex linear transforms, J. Math. Phys. 15 (8) (1974) 1295–1301.

[16] K.B. Wolf, On self-reciprocal functions under a class of integral transforms, J. Math. Phys. 18 (5) (1977) 1046–1051.
[17] A. Torre, Linear and radial canonical transforms of fractional order, J. Compt. Appl. Math. 153 (2003) 477–486.
[18] K.K. Sharma, Fractional laplace transform, Signal Image Video Process. 4 (3) (2009) 377–379.
[19] A.E. Siegman, Lasers, Mill Valley, California: University Science Books, 1986.
[20] D.F.V. James, G.S. Agarwal, The generalized Fresnel transform and its application to optics, Opt. Commun. 126 (4–6) (1996) 207–212.
[21] C. Palma, V. Bagini, Extension of the Fresnel transform to ABCD systems, J. Opt. Soc. Am. A 14 (8) (1997) 1774–1779.
[22] S. Abe, J.T. Sheridan, Generalization of the fractional Fourier transformation to an arbitrary linear lossless transformation an operator approach, J. Phys. A 27 (12) (1994) 4179–4187.
[23] S. Abe, J.T. Sheridan, Optical operations on wavefunctions as the Abelian subgroups of the special affine Fourier transformation, Opt. Lett. 19 (1994) 1801–1803.
[24] J. Hua, L. Liu, G. Li, Extended fractional Fourier transforms, J. Opt. Soc. Am. A 14 (12) (1997) 3316–3322.
[25] B. Davies, Integral Transforms and Their Applications, Springer, New York, 1978.
[26] A. Koç, F.S. Oktem, H.M. Ozaktas, M.A. Kutay, Fast Algorithms for Digital Computation of Linear Canonical Transforms, in: J.J. Healy, et al. (Eds.), Linear Canonical Transforms, Springer, New York, 2016, pp. 293–327.
[27] E. Hecht, Optics, 4th ed., Addison Wesley, 2001.
[28] M.J. Bastiaans, Wigner distribution function and its application to first-order optics, J. Opt. Soc. Am. 69 (1979) 1710–1716.
[29] H.M. Ozaktas, A. Koç, I. Sari, M.A. Kutay, Efficient computation of quadratic-phase integrals in optics, Opt. Lett. 31 (2006) 35–37.
[30] M. Moshinsky, Canonical transformations and quantum mechanics, SIAM J. Appl. Math. 25 (2) (1973) 193–212.
[31] C. Jung, H. Kruger, Representation of quantum mechanical wavefunctions by complex valued extensions of classical canonical transformation generators, J. Phys. A 15 (1982) 3509–3523.
[32] Q. Feng, B.-Z. Li, J.-M. Rassias, Weighted Heisenberg-Pauli-Weyl uncertainty principles for the linear canonical transform, Signal Process. 165 (2019) 209–221.
[33] B. Barshan, M.A. Kutay, H.M. Ozaktas, Optimal filtering with linear canonical transformations, Opt. Commun. 135 (1–3) (1997) 32–36.
[34] X. Chen, J. Guan, N. Liu, W. Zhou, Y. He, Detection of a low observable sea-surface target with micromotion via the Radon-linear canonical transform, IEEE Geosci. Remote Sensing Lett. 11 (7) (2014) 1225–1229.
[35] X. Chen, J. Guan, Y. Huang, N. Liu, Y. He, Radon-linear canonical ambiguity function-based detection and estimation method for marine target with micromotion, IEEE Trans. Geosci. Remote Sens. 53 (4) (2015) 2225–2240.
[36] W. Qiu, B.Z. Li, X.W. Li, Speech recovery based on the linear canonical transform, Speech Commun. 55 (1) (2013) 40–50.
[37] A. Koç, B. Bartan, E. Gundogdu, T. Çukur, H.M. Ozaktas, Sparse representation of two and three dimensional images with fractional Fourier, Hartley, linear canonical, and Haar wavelet transforms, Expert Syst. Appl. 77 (2017) 247–255.
[38] N. Singh, A. Sinha, Chaos based multiple image encryption using multiple canonical transforms, Opt. Laser Technol. 42 (2010) 724–731.
[39] B.Z. Li, Y.P. Shi, Image watermarking in the linear canonical transform domain, Math. Probl. Eng. (2014).
[40] M. Qi, B.-Z. Li, H. Sun, Image watermarking using polar harmonic transform with parameters in SL(2,R), Signal Process. Image Commun. 31 (2015) 161–173.
[41] M.J. Bastiaans, The Wigner distribution function applied to optical signals and systems, Opt. Commun. 25 (1) (1978) 26–30.
[42] T. Alieva, M.J. Bastiaans, Properties of the canonical integral transformation, J. Opt. Soc. Am. A 24 (2007) 3658–3665.
[43] M.J. Bastiaans, T. Alieva, Classification of lossless first-order optical systems and the linear canonical transformation, J. Opt. Soc. Am. A 24 (2007) 1053–1062.
[44] R. Simon, K.B. Wolf, Structure of the set of paraxial optical systems, J. Opt. Soc. Am. A 17 (2) (2000) 342–355.
[45] S.C. Pei, J.J. Ding, Closed-form discrete fractional and affine Fourier transforms, IEEE Trans. Signal Process. 48 (2000) 1338–1353.
[46] J. Zhao, R. Tao, Y. Wang, Sampling rate conversion for linear canonical transform, Signal Process. 88 (11) (2008) 2825–2832.
[47] A. Stern, Why is the linear canonical transform so little known? in: IP Conf. Proc., 2006, pp. 225–234.
[48] F. Zhang, R. Tao, Y. Wang, Discrete linear canonical transform computation by adaptive method, Opt. Express 21 (15) (2013) 18138–18151.
[49] A. Koç, H.M. Ozaktas, C. Candan, M.A. Kutay, Digital computation of linear canonical transforms, IEEE Trans. Signal Process. 56 (6) (2008) 2383–2394.
[50] F.S. Oktem, H.M. Ozaktas, Exact relation between continuous and discrete linear canonical transforms, Signal Process. Lett. IEEE 16 (8) (2009) 727–730.
[51] S.C. Pei, S. Huang, Fast discrete linear canonical transform based on CM-CC-CM decomposition and FFT, IEEE Trans. Signal Process. 64 (2016) 855–866.
[52] R.G. Campos, J. Figueroa, A fast algorithm for the linear canonical transform, Signal Process. 91 (6) (2011) 1444–1447.
[53] B.M. Hennelly, J.T. Sheridan, Fast numerical algorithm for the linear canonical transform, J. Opt. Soc. Am. A 22 (2005) 928–937.
[54] B.M. Hennelly, J.T. Sheridan, Generalizing, optimizing, and inventing numerical algorithms for the fractional Fourier, Fresnel, and linear canonical transforms, J. Opt. Soc. Am. A 22 (2005) 917–927.
[55] J.J. Healy, J.T. Sheridan, Sampling and discretization of the linear canonical transform, Signal Process. 89 (4) (2009) 641–648.
[56] J.J. Healy, J.T. Sheridan, Fast linear canonical transforms, J. Opt. Soc. Am. A 27 (1) (2010) 21–30.
[57] J.J. Healy, J.T. Sheridan, Reevaluation of the direct method of calculating Fresnel and other linear canonical transforms, Opt. Lett. 35 (7) (2010) 947–949.
[58] S.C. Pei, Y.C. Lai, Discrete linear canonical transforms based on dilated Hermite functions, J. Opt. Soc. Am. A 28 (8) (2011) 1695–1708.
[59] L. Zhao, J.J. Healy, J.T. Sheridan, Unitary discrete linear canonical transform: analysis and application, Appl. Opt. 52 (7) (2013) C30–C36.
[60] D. Wei, R. Wang, Y.-M. Li, Random discrete linear canonical transform, J. Opt. Soc. Am. A 33 (12) (2016) 2470–2476.
[61] A. Koç, B. Bartan, H.M. Ozaktas, Discrete linear canonical transform based on hyperdifferential operators, IEEE Trans. Signal Process. 67 (9) (2019) 2237–2248.
[62] C. Candan, M.A. Kutay, H.M. Ozaktas, The discrete fractional Fourier transform, IEEE Trans. Signal Process. 48 (5) (2000) 1329–1337.
[63] K.B. Wolf, Finite systems, fractional Fourier transforms and their finite phase spaces, Czech. J. Phys. 55 (2005) 1527–1534.
[64] K.B. Wolf, G. Krötzsch, Geometry and dynamics in the fractional discrete Fourier transform, J. Opt. Soc. Am. A 24 (3) (2007) 651–658.
[65] S.C. Pei, M.H. Yeh, Improved discrete fractional Fourier transform, Opt Lett. 22 (14) (1997) 1047–1049.
[66] N.M. Atakishiyev, L.E. Vicent, K.B. Wolf, Continuous vs. discrete fractional Fourier transforms, J. Comput. Appl. Math. 107 (1) (1999) 73–95.
[67] S.C. Pei, M.H. Yeh, C.C. Tseng, Discrete fractional Fourier transform based on orthogonal projections, IEEE Trans. Signal Process. 47 (5) (1999) 1335–1348.
[68] A.I. Zayed, A.G. Garcia, New sampling formulae for the fractional Fourier transform, Signal Process. 77 (1) (1999) 111–114.
[69] M.H. Yeh, Angular decompositions for the discrete fractional signal transforms, Signal Process. 85 (3) (2005) 537–547.
[70] T. Erseghe, P. Kraniauskas, G. Carioraro, Unified fractional Fourier transform and sampling theorem, Signal Process. IEEE Trans. 47 (12) (1999) 3419–3423.
[71] A. Koç, Operator theory-based discrete fractional Fourier transform, Signal Image Video Process. 13 (7) (2019) 1461–1468.
[72] X. Su, R. Tao, X. Kang, Analysis and comparison of discrete fractional Fourier transforms, Signal Process. 160 (2019) 284–298.
[73] H. Zhang, T. Shan, S. Liu, R. Tao, Optimized sparse fractional Fourier transform: principle and performance analysis, Signal Process. 174 (2020) 107646.
[74] J.R. de Oliveira Neto, J.B. Lima, G.J.d. Silva, R.M.C. de Souza, Computation of an eigendecomposition-based discrete fractional Fourier transform with reduced arithmetic complexity, Signal Process. 165 (2019) 72–82.
[75] H. Zhao, L. Qiao, N. Fu, G. Huang, A generalized sampling model in shift-invariant spaces associated with fractional fourier transform, Signal Process. 145 (2018) 1–11.
[76] D. Gottlieb, M.Y. Hussaini, S.A. Orszag, Spectral Methods for Partial Differential Equations (Chapter: Introduction - Theory and Applications of Spectral Methods), SIAM, Philadelphia, PA, 1984.